

Measurement of the High-Mass Drell-Yan Cross Section and Limits on Quark-Electron Compositeness Scales

B. Abbott,⁴⁰ M. Abolins,³⁷ V. Abramov,¹⁵ B. S. Acharya,⁸ I. Adam,³⁹ D. L. Adams,⁴⁹ M. Adams,²⁴ S. Ahn,²³ H. Aihara,¹⁷ G. A. Alves,² N. Amos,³⁶ E. W. Anderson,³⁰ M. M. Baarmand,⁴² V. V. Babintsev,¹⁵ L. Babukhadia,¹⁶ A. Baden,³³ B. Baldin,²³ S. Banerjee,⁸ J. Bantly,⁴⁶ E. Barberis,¹⁷ P. Baringer,³¹ J. F. Bartlett,²³ A. Belyaev,¹⁴ S. B. Beri,⁶ I. Bertram,²⁶ V. A. Bezzubov,¹⁵ P. C. Bhat,²³ V. Bhatnagar,⁶ M. Bhattacharjee,⁴² N. Biswas,²⁸ G. Blazey,²⁵ S. Blessing,²¹ P. Bloom,¹⁸ A. Boehnlein,²³ N. I. Bojko,¹⁵ F. Borchering,²³ C. Boswell,²⁰ A. Brandt,²³ R. Breedon,¹⁸ R. Brock,³⁷ A. Bross,²³ D. Buchholz,²⁶ V. S. Burtovoi,¹⁵ J. M. Butler,³⁴ W. Carvalho,² D. Casey,³⁷ Z. Casilum,⁴² H. Castilla-Valdez,¹¹ D. Chakraborty,⁴² S.-M. Chang,³⁵ S. V. Chekulaev,¹⁵ W. Chen,⁴² S. Choi,¹⁰ S. Chopra,³⁶ B. C. Choudhary,²⁰ J. H. Christenson,²³ M. Chung,²⁴ D. Claes,³⁸ A. R. Clark,¹⁷ W. G. Cobau,³³ J. Cochran,²⁰ L. Coney,²⁸ W. E. Cooper,²³ C. Cretsinger,⁴¹ D. Cullen-Vidal,⁴⁶ M. A. C. Cummings,²⁵ D. Cutts,⁴⁶ O. I. Dahl,¹⁷ K. Davis,¹⁶ K. De,⁴⁷ K. Del Signore,³⁶ M. Demarteau,²³ D. Denisov,²³ S. P. Denisov,¹⁵ H. T. Diehl,²³ M. Diesburg,²³ G. Di Loreto,³⁷ P. Draper,⁴⁷ Y. Ducros,⁵ L. V. Dudko,¹⁴ S. R. Dugad,⁸ A. Dyshkant,¹⁵ D. Edmunds,³⁷ J. Ellison,²⁰ V. D. Elvira,⁴² R. Engelmann,⁴² S. Eno,³³ G. Eppley,⁴⁹ P. Ermolov,¹⁴ O. V. Eroshin,¹⁵ V. N. Evdokimov,¹⁵ T. Fahland,¹⁹ M. K. Fatyga,⁴¹ S. Feher,²³ D. Fein,¹⁶ T. Ferbel,⁴¹ G. Finocchiaro,⁴² H. E. Fisk,²³ Y. Fisyaik,⁴³ E. Flattum,²³ G. E. Forden,¹⁶ M. Fortner,²⁵ K. C. Frame,³⁷ S. Fuess,²³ E. Gallas,⁴⁷ A. N. Galyaev,¹⁵ P. Gartung,²⁰ V. Gavrilov,¹³ T. L. Geld,³⁷ R. J. Genik II,³⁷ K. Genser,²³ C. E. Gerber,²³ Y. Gershtein,¹³ B. Gibbard,⁴³ B. Gobbi,²⁶ B. Gómez,⁴ G. Gómez,³³ P. I. Goncharov,¹⁵ J. L. González Solís,¹¹ H. Gordon,⁴³ L. T. Goss,⁴⁸ K. Gounder,²⁰ A. Goussiou,⁴² N. Graf,⁴³ P. D. Grannis,⁴² D. R. Green,²³ H. Greenlee,²³ S. Grinstein,¹ P. Grudberg,¹⁷ S. Grünendahl,²³ G. Guglielmo,⁴⁵ J. A. Guida,¹⁶ J. M. Guida,⁴⁶ A. Gupta,⁸ S. N. Gurzhiev,¹⁵ G. Gutierrez,²³ P. Gutierrez,⁴⁵ N. J. Hadley,³³ H. Haggerty,²³ S. Hagopian,²¹ V. Hagopian,²¹ K. S. Hahn,⁴¹ R. E. Hall,¹⁹ P. Hanlet,³⁵ S. Hansen,²³ J. M. Hauptman,³⁰ D. Hedin,²⁵ A. P. Heinson,²⁰ U. Heintz,²³ R. Hernández-Montoya,¹¹ T. Heuring,²¹ R. Hirosky,²⁴ J. D. Hobbs,⁴² B. Hoeneisen,^{4,*} J. S. Hoftun,⁴⁶ F. Hsieh,³⁶ Tong Hu,²⁷ A. S. Ito,²³ J. Jaques,²⁸ S. A. Jerger,³⁷ R. Jesik,²⁷ T. Joffe-Minor,²⁶ K. Johns,¹⁶ M. Johnson,²³ A. Jonckheere,²³ M. Jones,²² H. Jöstlein,²³ S. Y. Jun,²⁶ C. K. Jung,⁴² S. Kahn,⁴³ G. Kalbfleisch,⁴⁵ D. Karmanov,¹⁴ D. Karmgard,²¹ R. Kehoe,²⁸ M. L. Kelly,²⁸ S. K. Kim,¹⁰ B. Klima,²³ C. Klopfenstein,¹⁸ W. Ko,¹⁸ J. M. Kohli,⁶ D. Koltick,²⁹ A. V. Kostitskiy,¹⁵ J. Kotcher,⁴³ A. V. Kotwal,³⁹ A. V. Kozelov,¹⁵ E. A. Kozlovsky,¹⁵ J. Krane,³⁸ M. R. Krishnaswamy,⁸ S. Krzywdzinski,²³ S. Kuleshov,¹³ Y. Kulik,⁴² S. Kunori,³³ F. Landry,³⁷ G. Landsberg,⁴⁶ B. Lauer,³⁰ A. Leflat,¹⁴ J. Li,⁴⁷ Q. Z. Li,²³ J. G. R. Lima,³ D. Lincoln,²³ S. L. Linn,²¹ J. Linnemann,³⁷ R. Lipton,²³ F. Lobkowicz,⁴¹ S. C. Loken,¹⁷ A. Lucotte,⁴² L. Lueking,²³ A. L. Lyon,³³ A. K. A. Maciel,² R. J. Madaras,¹⁷ R. Madden,²¹ L. Magaña-Mendoza,¹¹ V. Manankov,¹⁴ S. Mani,¹⁸ H. S. Mao,^{23,†} R. Markeloff,²⁵ T. Marshall,²⁷ M. I. Martin,²³ K. M. Mauritz,³⁰ B. May,²⁶ A. A. Mayorov,¹⁵ R. McCarthy,⁴² J. McDonald,²¹ T. McKibben,²⁴ J. McKinley,³⁷ T. McMahon,⁴⁴ H. L. Melanson,²³ M. Merkin,¹⁴ K. W. Merritt,²³ C. Miao,⁴⁶ H. Miettinen,⁴⁹ A. Mincer,⁴⁰ C. S. Mishra,²³ N. Mokhov,²³ N. K. Mondal,⁸ H. E. Montgomery,²³ P. Mooney,⁴ M. Mostafa,¹ H. da Motta,² C. Murphy,²⁴ F. Nang,¹⁶ M. Narain,²³ V. S. Narasimham,⁸ A. Narayanan,¹⁶ H. A. Neal,³⁶ J. P. Negret,⁴ P. Nemethy,⁴⁰ D. Norman,⁴⁸ L. Oesch,³⁶ V. Oguri,³ E. Oliveira,² E. Oltman,¹⁷ N. Oshima,²³ D. Owen,³⁷ P. Padley,⁴⁹ A. Para,²³ Y. M. Park,⁹ R. Partridge,⁴⁶ N. Parua,⁸ M. Paterno,⁴¹ B. Pawlik,¹² J. Perkins,⁴⁷ M. Peters,²² R. Piegaia,¹ H. Piekarz,²¹ Y. Pischalnikov,²⁹ B. G. Pope,³⁷ H. B. Prosper,²¹ S. Protopopescu,⁴³ J. Qian,³⁶ P. Z. Quintas,²³ R. Raja,²³ S. Rajagopalan,⁴³ O. Ramirez,²⁴ S. Reucroft,³⁵ M. Rijssenbeek,⁴² T. Rockwell,³⁷ M. Roco,²³ P. Rubinov,²⁶ R. Ruchti,²⁸ J. Rutherford,¹⁶ A. Sánchez-Hernández,¹¹ A. Santoro,² L. Sawyer,³² R. D. Schamberger,⁴² H. Schellman,²⁶ J. Sculli,⁴⁰ E. Shabalina,¹⁴ C. Shaffer,²¹ H. C. Shankar,⁸ R. K. Shivpuri,⁷ D. Shpakov,⁴² M. Shupe,¹⁶ H. Singh,²⁰ J. B. Singh,⁶ V. Sirotenko,²⁵ E. Smith,⁴⁵ R. P. Smith,²³ R. Snihur,²⁶ G. R. Snow,³⁸ J. Snow,⁴⁴ S. Snyder,⁴³ J. Solomon,²⁴ M. Sosebee,⁴⁷ N. Sotnikova,¹⁴ M. Souza,² G. Steinbrück,⁴⁵ R. W. Stephens,⁴⁷ M. L. Stevenson,¹⁷ F. Stichelbaut,⁴² D. Stoker,¹⁹ V. Stolin,¹³ D. A. Stoyanova,¹⁵ M. Strauss,⁴⁵ K. Streets,⁴⁰ M. Strovink,¹⁷ A. Sznajder,² P. Tamburello,³³ J. Tarazi,¹⁹ M. Tartaglia,²³ T. L. T. Thomas,²⁶ J. Thompson,³³ T. G. Trippe,¹⁷ P. M. Tuts,³⁹ V. Vaniev,¹⁵ N. Varelas,²⁴ E. W. Varnes,¹⁷ D. Vititoe,¹⁶ A. A. Volkov,¹⁵ A. P. Vorobiev,¹⁵ H. D. Wahl,²¹ G. Wang,²¹ J. Warchol,²⁸ G. Watts,⁴⁶ M. Wayne,²⁸ H. Weerts,³⁷ A. White,⁴⁷ J. T. White,⁴⁸ J. A. Wightman,³⁰ S. Willis,²⁵ S. J. Wimpenny,²⁰ J. V. D. Wirjawan,⁴⁸ J. Womersley,²³ E. Won,⁴¹ D. R. Wood,³⁵ Z. Wu,^{23,†} R. Yamada,²³ P. Yamin,⁴³ T. Yasuda,³⁵ P. Yepes,⁴⁹ K. Yip,²³ C. Yoshikawa,²² S. Youssef,²¹ J. Yu,²³ Y. Yu,¹⁰ B. Zhang,^{23,†} Y. Zhou,^{23,†} Z. Zhou,³⁰ Z. H. Zhu,⁴¹ M. Zielinski,⁴¹ D. Zieminska,²⁷ A. Zieminski,²⁷ E. G. Zverev,¹⁴ and A. Zylberstejn⁵

(D0 Collaboration)

- ¹*Universidad de Buenos Aires, Buenos Aires, Argentina*
²*LAFEX, Centro Brasileiro de Pesquisas Físicas, Rio de Janeiro, Brazil*
³*Universidade do Estado do Rio de Janeiro, Rio de Janeiro, Brazil*
⁴*Universidad de los Andes, Bogotá, Colombia*
⁵*DAPNIA/Service de Physique des Particules, CEA, Saclay, France*
⁶*Panjab University, Chandigarh, India*
⁷*Delhi University, Delhi, India*
⁸*Tata Institute of Fundamental Research, Mumbai, India*
⁹*Kyungshung University, Pusan, Korea*
¹⁰*Seoul National University, Seoul, Korea*
¹¹*CINVESTAV, Mexico City, Mexico*
¹²*Institute of Nuclear Physics, Kraków, Poland*
¹³*Institute for Theoretical and Experimental Physics, Moscow, Russia*
¹⁴*Moscow State University, Moscow, Russia*
¹⁵*Institute for High Energy Physics, Protvino, Russia*
¹⁶*University of Arizona, Tucson, Arizona 85721*
¹⁷*Lawrence Berkeley National Laboratory and University of California, Berkeley, California 94720*
¹⁸*University of California, Davis, California 95616*
¹⁹*University of California, Irvine, California 92697*
²⁰*University of California, Riverside, California 92521*
²¹*Florida State University, Tallahassee, Florida 32306*
²²*University of Hawaii, Honolulu, Hawaii 96822*
²³*Fermi National Accelerator Laboratory, Batavia, Illinois 60510*
²⁴*University of Illinois at Chicago, Chicago, Illinois 60607*
²⁵*Northern Illinois University, DeKalb, Illinois 60115*
²⁶*Northwestern University, Evanston, Illinois 60208*
²⁷*Indiana University, Bloomington, Indiana 47405*
²⁸*University of Notre Dame, Notre Dame, Indiana 46556*
²⁹*Purdue University, West Lafayette, Indiana 47907*
³⁰*Iowa State University, Ames, Iowa 50011*
³¹*University of Kansas, Lawrence, Kansas 66045*
³²*Louisiana Tech University, Ruston, Louisiana 71272*
³³*University of Maryland, College Park, Maryland 20742*
³⁴*Boston University, Boston, Massachusetts 02215*
³⁵*Northeastern University, Boston, Massachusetts 02115*
³⁶*University of Michigan, Ann Arbor, Michigan 48109*
³⁷*Michigan State University, East Lansing, Michigan 48824*
³⁸*University of Nebraska, Lincoln, Nebraska 68588*
³⁹*Columbia University, New York, New York 10027*
⁴⁰*New York University, New York, New York 10003*
⁴¹*University of Rochester, Rochester, New York 14627*
⁴²*State University of New York, Stony Brook, New York 11794*
⁴³*Brookhaven National Laboratory, Upton, New York 11973*
⁴⁴*Langston University, Langston, Oklahoma 73050*
⁴⁵*University of Oklahoma, Norman, Oklahoma 73019*
⁴⁶*Brown University, Providence, Rhode Island 02912*
⁴⁷*University of Texas, Arlington, Texas 76019*
⁴⁸*Texas A&M University, College Station, Texas 77843*
⁴⁹*Rice University, Houston, Texas 77005*

(Received 7 December 1998)

We present a measurement of the Drell-Yan cross section at high dielectron invariant mass using 120 pb^{-1} of data collected in $p\bar{p}$ collisions at $\sqrt{s} = 1.8 \text{ TeV}$ by the D0 Collaboration during 1992–1996. No deviation from standard model expectations is observed. We use the data to set limits on the quark-electron compositeness scale. The 95% confidence level lower limits on the compositeness scale vary between 3.3 and 6.1 TeV depending on the assumed form of the effective contact interaction. [S0031-9007(99)09217-0]

PACS numbers: 12.60.Rc, 13.85.Qk

In $p\bar{p}$ collisions, e^+e^- pairs can be produced through the Drell-Yan process [1] over a large range in their invariant mass. In the standard model (SM), the process occurs to first order via quark-antiquark annihilation into a virtual photon or virtual (and real) Z boson. The measurement of the Drell-Yan cross section at the Tevatron constrains possible new physics beyond the standard model. Aside from the main motivation of the search for composite quarks and leptons, the measurement has broader interest in that it can constrain the existence of any new boson

$$\mathcal{L} = \frac{4\pi}{\Lambda^2} [\eta_{LL}(\bar{q}_L\gamma^\mu q_L)(\bar{e}_L\gamma_\mu e_L) + \eta_{LR}(\bar{q}_L\gamma^\mu q_L)(\bar{e}_R\gamma_\mu e_R) + \eta_{RL}(\bar{q}_R\gamma^\mu q_R)(\bar{e}_L\gamma_\mu e_L) + \eta_{RR}(\bar{q}_R\gamma^\mu q_R)(\bar{e}_R\gamma_\mu e_R)],$$

where $q = (u, d)$ represents the first generation quarks, Λ is the compositeness scale, $\eta_{ij} = \pm 1$, and L (R) denotes the left (right) helicity projection. The addition of this contact term to the SM Lagrangian modifies the γ/Z boson production cross section, with the largest effects expected at high e^+e^- invariant mass. Composite quarks and electrons have been proposed as a possible explanation of the high- Q^2 anomaly at HERA [5]. Previous results on quark-electron compositeness set lower limits on the compositeness scale Λ in the range of 2.5–5.2 TeV [6] and 2.1–3.5 TeV [7]. In this Letter, we report the measurement of the Drell-Yan cross section at high mass and set the most stringent limits to date on the quark-electron compositeness scale.

The results presented here used 120 pb⁻¹ of data collected in $p\bar{p}$ collisions at $\sqrt{s} = 1.8$ TeV by the D0 detector [8] during the 1992–1996 run at the Fermilab Tevatron. The detector consists of a tracking system, a highly linear, granular and stable uranium/liquid-argon calorimeter, and a muon spectrometer. The D0 detector does not have a central magnetic field and consequently cannot distinguish between the charges of the e^+ and e^- . Electron candidates are accepted in the pseudorapidity range of $|\eta| < 1.1$ for electrons detected in the central calorimeter (CC) and $1.5 < |\eta| < 2.5$ for electrons detected in the forward calorimeters (EC), where $\eta = -\log \tan(\theta/2)$ and θ is the polar angle with respect to the beam axis. CC electrons within 0.0098 radians in azimuth of any calorimeter module edge are removed to ensure uniform calorimeter response. At least two electrons were required to have $E_T > 20$ GeV at the trigger level. For full trigger efficiency, an off-line kinematic requirement of $E_T > 25$ GeV is applied on the two highest- E_T electrons in the event.

Off-line, a “loose” electron must satisfy three requirements: (1) The electron must deposit at least 95% of its energy in the electromagnetic calorimeter, (ii) the transverse and longitudinal shower shapes must be consistent with those expected for an electron, and (iii) the electron must be isolated in a cone of radius $R = \sqrt{\Delta\eta^2 + \Delta\phi^2} = 0.4$, such that $\frac{E_{\text{tot}}(R=0.4) - E_{\text{EM}}(R=0.2)}{E_{\text{EM}}(R=0.2)} < 0.15$, where E_{tot} and E_{EM}

possessing Yukawa couplings to quarks and leptons. It is therefore relevant to ongoing searches for compositeness at e^+e^- and ep colliders and is complementary to low-energy experiments on parity violation in atoms [2].

If quarks and leptons are composite, with at least one constituent that is common to both of them, the interaction of these constituents would likely be manifested through an effective four fermion contact interaction at energies below the compositeness scale. We consider a general contact-interaction Lagrangian [3,4] of the form

are the total and EM calorimeter energies, respectively. A “tight” electron is additionally required to have a matching track in the drift chambers. In this analysis, any forward electron is required to be tight and at least one member of each electron pair must be tight.

The detector acceptance for dielectron events is defined as the fraction of produced events in which both electrons pass our kinematic and fiducial cuts. To calculate the acceptance, Drell-Yan events are generated using PYTHIA [9]. The parton showering parameters in PYTHIA were tuned for good kinematic modeling of the data using the distribution of the Z boson transverse momentum (p_T) observed at D0. The detector response is simulated using a parametrized Monte Carlo program [10]. The sampling and noise terms in the electron energy resolution are derived from test beam data and the calorimeter pedestal distribution in $W \rightarrow e\nu$ collider data, respectively. The constant term is constrained by the observed width of the $Z \rightarrow ee$ mass peak. The known Z boson mass is used to set the electromagnetic energy scale.

The acceptance, calculated using the Drell-Yan Monte Carlo model and MRS(A') [11] parton distribution functions, is $\approx 53\%$ and does not depend strongly on mass above $m_{ee} = 250$ GeV/ c^2 . This makes the analysis relatively model independent. The systematic uncertainty on the acceptance due to the production model is estimated to be 1.5%. The effect of energy smearing, included in the acceptance calculation, is small because the energy resolution ($15\%/\sqrt{E(\text{GeV})} \oplus 1\%$) is much smaller than the bin width at high mass.

The electron trigger and off-line selection efficiencies are determined using $Z \rightarrow ee$ data. One of the electrons is required to satisfy the tight selection criteria. The second electron then provides an unbiased sample to measure the efficiencies. Background subtraction is performed using the sidebands of the Z boson mass distribution. The trigger is found to be fully efficient for high mass dielectrons ($m_{ee} > 120$ GeV/ c^2). The single-electron efficiency for the CC loose selection criteria is $(92.9 \pm 0.7)\%$ and for the tight selection criteria is $(74.1 \pm 0.6)\%$. The efficiency for EC tight selection criteria is $(52.6 \pm 1.0)\%$.

TABLE I. The observed number of events N , total detection efficiency, expected total background, and the dielectron production cross section in the given mass bins. In the three highest mass bins, we quote the 95% (84%) C.L. upper limits on the cross section. The last column gives the value \tilde{m} of mass at which, for a NNLO SM calculation, $d\sigma^{\text{th}}/dm$ equals $\sigma^{\text{th}}/\Delta m$. Here σ^{th} denotes the total theoretical cross section in the bin and Δm denotes the bin width.

m_{ee} bin (GeV/ c^2)	N	Total efficiency	Expected background	σ (pb)	\tilde{m} (GeV/ c^2)
120–160	136	0.32 ± 0.01	64.0 ± 10.0	$1.93^{+0.43}_{-0.44}$	135
160–200	38	0.34 ± 0.01	22.0 ± 3.5	$0.49^{+0.16}_{-0.18}$	177
200–240	18	0.36 ± 0.01	6.34 ± 0.96	$0.28^{+0.09}_{-0.10}$	218
240–290	7	0.37 ± 0.01	3.61 ± 0.56	$0.066^{+0.052}_{-0.058}$	262
290–340	2	0.38 ± 0.01	1.37 ± 0.23	$0.033^{+0.032}_{-0.030}$	312
340–400	4	0.39 ± 0.01	0.75 ± 0.13	$0.057^{+0.042}_{-0.047}$	367
400–500	0	0.40 ± 0.01	0.23 ± 0.04	<0.063 (0.039)	443
500–600	0	0.41 ± 0.01	0.06 ± 0.02	<0.060 (0.037)	544
600–1000	0	0.42 ± 0.01	0.03 ± 0.01	<0.058 (0.035)	729

The dependence of dielectron selection efficiency on invariant mass was studied using a detailed GEANT-based Monte Carlo [12] simulation of dielectron events. There was no observed dependence of selection efficiency on dielectron mass.

The most important sources of background to $p\bar{p} \rightarrow ee + X$ are QCD multijet events with two jets misidentified as electrons and direct-photon events where both the photon and a jet are misidentified as electrons. Jets with a leading π^0 or η may produce an isolated and energetic photon that passes the loose or tight electron selection criteria, depending on the presence of an associated track. Using multijet and photon-jet data samples, the probability for misidentifying a jet as an electron is measured as a function of jet E_T . A CC jet with $E_T = 100$ GeV is misidentified as a tight electron with a probability of 0.8×10^{-3} and as a loose electron with a probability of 1.8×10^{-3} . An EC jet with $E_T = 100$ GeV is misidentified as a tight electron with a probability of 1.0×10^{-3} . The uncertainty on these estimated probabilities is of the order of 25%, which is dominated by the uncertainty in the direct-photon fraction of the data samples used. Estimated backgrounds to the dielectron sample from multijet, photon-jet, and $W + \text{jet}$ sources were calculated independently as a function of mass by weighting the total number of dijet, photon-jet, and $W + \text{jet}$ pairs in any given mass bin by the appropriate misidentification probability and sample luminosities. The uncertainty on these estimated backgrounds is due to the systematic uncertainty on the misidentification probability and the statistics of dijet, photon-jet, and $W + \text{jet}$ samples.

In addition to misidentification backgrounds, other high p_T processes contribute to dielectron final states. We use PYTHIA Monte Carlo events, passed through the parametrized detector simulation, to estimate these backgrounds. Since electrons and photons will pass the loose electron selection cuts, we evaluated five possible back-

ground processes, $W\gamma \rightarrow e\nu\gamma$, $Z\gamma \rightarrow ee\gamma$, $t\bar{t} \rightarrow eeX$, $WW \rightarrow eeX$, and $\gamma^*/Z \rightarrow \tau\tau \rightarrow eeX$, and found them to contribute less than 10% of the total background.

The measurement of the inclusive dielectron cross section is performed in independent mass bins using a Bayesian [13] technique. In each bin k , we determine the posterior probability density $P(\sigma^k | N_o^k)$ for the cross section σ^k , given the observed number of events N_o^k . The expected number of events in the k^{th} mass bin is given by $N^k = b^k + \mathcal{L}\epsilon^k\sigma^k$, where b^k is the expected background, \mathcal{L} is the luminosity, ϵ^k is the total signal efficiency (including acceptance, selection efficiency, and smearing correction), and σ^k is the total cross section in that bin. The posterior probability density for the cross

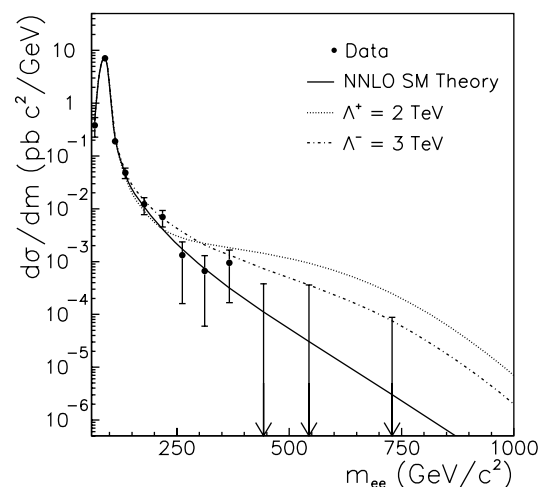


FIG. 1. The differential inclusive dielectron production cross section. The 68% uncertainty intervals are shown for the data points. The last three bins, which have no events, show the 84% C.L. upper limit on the cross section corresponding to the upper end of the error bars in the preceding bins. Also shown is the prediction of the SM at NNLO, and SM + contact term process at LO corrected with a NNLO K factor.

TABLE II. 95% C.L. lower limit on the scale of compositeness Λ in TeV for different contact interaction models. The superscript on Λ indicates the sign of η_{ij} , which governs the nature of the interference (negative sign for constructive interference) between the contact interaction and the SM Lagrangian.

	LL	LR	RL	RR	$LL + RR$	$LR + RL$	$LL - LR$	$RL - RR$	VV	AA
Λ^+ (TeV)	3.3	3.4	3.3	3.3	4.2	3.9	3.9	4.0	4.9	4.7
Λ^- (TeV)	4.2	3.6	3.7	4.0	5.1	4.4	4.5	4.3	6.1	5.5

section σ^k is

$$P(\sigma^k | N_o^k) = \frac{1}{A} \int db d\mathcal{L} d\epsilon \frac{e^{-N^k} N^k N_o^{k_0}}{N_o^{k_0}!} P(b^k, \mathcal{L}, \epsilon^k) P(\sigma^k),$$

where A is the normalization. The prior probability density $P(b, \mathcal{L}, \epsilon)$ is taken to be a product of independent Gaussian distributions in b , \mathcal{L} , and ϵ , with the measured value in each bin defining the mean and the uncertainty defining the width. The prior distribution $P(\sigma^k)$ in any bin is chosen to be uniform in σ . The measured value of the cross section for each bin is taken to be the mode of the posterior probability density (maximum likelihood estimate). The interval of minimum width containing 68% of the area defines the uncertainty on the cross section. Table I shows the observed number of events, the product of detector acceptance and efficiency, and the expected background for dielectron events. The second-to-last column shows the measured dielectron cross section and the associated uncertainty, dominated by event statistics in the high-mass bins. In bins with no observed events, we quote the 95% and 84% confidence level (C.L.) upper limits on the cross section, defined by $\int_0^\sigma P(\sigma' | N_o) d\sigma' = 0.95$ (0.84). The measured differential cross sections $d\sigma/dm$ are compared with predictions of a next-to-next-to-leading order (NNLO) SM calculation [14] in Fig. 1. We find no significant deviation between the measurement and theory. The figure also illustrates the expected distribution of the dielectron cross section with the inclusion of contact term processes with the SM.

To set limits on the compositeness scale Λ , we calculate the cross section for the Drell-Yan + contact term process by including terms from the contact interaction Lagrangian [3,4] with the SM Lagrangian. We correct the leading order (LO) cross section calculation for higher order QCD effects using a mass-dependent K factor. The K factor is defined as the ratio of the NNLO Drell-Yan cross section calculation from Ref. [14] to our calculated LO Drell-Yan cross section. Limits are set independently for each separate channel of the contact-interaction Lagrangian: LL , LR , RL , and RR , and $\eta_{ij} = \pm 1$. The first letter indicates the helicity of the quark current and the second letter indicates the helicity of the lepton current. These terms are strongly constrained by atomic parity-violation measurements (APV) [15], implying $\Lambda > 10$ TeV. However, parity conserving or other symmetric combinations of these terms, such as $LL + RR$, $LR + RL$

[16,17], $LL - LR$, $RL - RR$ [18], vector-vector ($VV = LL + RR + LR + RL$) [19], and axial vector-axial vector ($AA = LL + RR - LR - RL$) [19,20], are not constrained by APV. Our measurements impose strong constraints on all of these models.

The limit on the quark-electron compositeness scale is calculated using a Bayesian analysis of the shape of the mass distribution of events. The expected number of events in the k^{th} mass bin is denoted by $N_\Lambda^k = b^k + \mathcal{L} \epsilon^k \sigma_\Lambda^k$, where σ_Λ^k is the predicted cross section including compositeness ($\Lambda \rightarrow \infty$ gives the SM cross section). To reduce the normalization uncertainty in the theory for the limit-setting analysis, the SM prediction for the number of events in the Z boson mass bin is normalized to the observed number of events. The posterior probability density for the compositeness scale Λ , given the observed data distribution (D), is given by

$$P(\Lambda | D) = \frac{1}{A} \int db d\epsilon \prod_{k=1}^n \left[\frac{e^{-N_\Lambda^k} N_\Lambda^k N_o^{k_0}}{N_o^{k_0}!} P(b^k, \epsilon^k) \right] P(\Lambda).$$

The bin-to-bin correlations in the value and the uncertainty on the background are taken into account. In accordance with the convention [6,7,17], the prior distribution $P(\Lambda)$ is chosen to be uniform in $1/\Lambda^2$. This represents a prior approximately uniform in cross section. The resulting posterior density $P(\Lambda | D)$ peaks at $1/\Lambda^2 = 0$ and falls monotonically with increasing $1/\Lambda^2$. The 95% C.L. lower limit is defined by $\int_\Lambda^\infty P(\Lambda' | D) d\Lambda' = 0.95$. The limits for various helicity options are shown in Table II. Other choices of prior distributions result in 5%–8% variation of these limits.

In conclusion, we have measured the differential cross section for dielectron pair production at high dielectron mass. We find no significant deviation from the SM. We have used the data to set limits on the quark-electron compositeness scale in the context of an effective contact interaction. In the chiral channels (i.e., either the quark or the lepton current is not vector or axial-vector), the 95% C.L. lower limits on Λ^+ vary between 3.3 and 4.2 TeV, and limits on Λ^- vary between 3.6 and 5.1 TeV. The VV and AA limits are more stringent, varying between 4.7 and 4.9 TeV for Λ^+ and 5.5 and 6.1 TeV for Λ^- . These are the best limits to date on quark-electron compositeness and are fairly independent of the helicity structure of the contact interaction.

We thank T. Sjöstrand for discussions regarding PYTHIA and W.L. Van Neerven for providing the code to compute the NNLO SM Drell-Yan cross section. We thank the staffs at Fermilab and collaborating institutions for their contributions to this work and acknowledge support from the Department of Energy and National Science Foundation (U.S.A.), Commissariat à L'Energie Atomique (France), Ministry for Science and Technology and Ministry for Atomic Energy (Russia), CAPES and CNPq (Brazil), Departments of Atomic Energy and Science and Education (India), Colciencias (Colombia), CONACyT (Mexico), Ministry of Education and KOSEF (Korea), and CONICET and UBACyT (Argentina).

*Visitor from Universidad San Francisco de Quito, Quito, Ecuador.

†Visitor from IHEP, Beijing, China.

- [1] S. D. Drell and T. M. Yan, *Phys. Rev. Lett.* **25**, 316 (1970).
- [2] C. S. Wood *et al.*, *Science* **275**, 1759 (1997).
- [3] E. Eichten, K. Lane, and M. Peskin, *Phys. Rev. Lett.* **50**, 811 (1983); E. Eichten, I. Hinchliffe, K. Lane, and C. Quigg, *Rev. Mod. Phys.* **56**, 4 (1984).
- [4] T. Lee, *Phys. Rev. D* **55**, 2591 (1997).
- [5] H1 Collaboration, C. Adloff *et al.*, *Z. Phys. C* **74**, 191 (1997); ZEUS Collaboration, J. Breitweg *et al.*, *Z. Phys. C* **74**, 207 (1997).
- [6] CDF Collaboration, F. Abe *et al.*, *Phys. Rev. Lett.* **79**, 2198 (1997).
- [7] OPAL Collaboration, K. Ackerstaff *et al.*, *Phys. Lett. B* **391**, 221 (1997).
- [8] D0 Collaboration, S. Abachi *et al.*, *Nucl. Instrum. Methods Phys. Res., Sect. A* **338**, 185 (1994).
- [9] T. Sjöstrand, *Comput. Phys. Commun.* **82**, 74 (1994).
- [10] D0 Collaboration, B. Abbott *et al.*, *Phys. Rev. D* **58**, 092003 (1998).
- [11] A. D. Martin, R. G. Roberts, and W. J. Stirling, *Phys. Rev. D* **50**, 6734 (1994); **51**, 4756 (1995).
- [12] F. Carminati *et al.*, "GEANT Users Guide V3.14," CERN Library Writeup W5013, 1993 (unpublished).
- [13] E. T. Jaynes, *Probability Theory: The Logic of Science*, <ftp://bayes.wustl.edu/pub/Jaynes/book.probability.theory/> (unpublished).
- [14] R. Hamberg, W.L. Van Neerven, and T. Matsuura, *Nucl. Phys.* **B359**, 343 (1991).
- [15] P. Langacker, *Phys. Lett. B* **256**, 277 (1991); M. Leurer, *Phys. Rev. D* **49**, 333 (1994).
- [16] K. S. Babu, C. Kolda, J. March-Russell, and F. Wilczek, *Phys. Lett. B* **402**, 367 (1997).
- [17] V. Barger, K. Cheung, K. Hagiwara, and D. Zeppenfeld, *Phys. Lett. B* **404**, 147 (1997).
- [18] A. Nelson, *Phys. Rev. Lett.* **78**, 4159 (1997).
- [19] N. Bartolomeo and M. Fabbrichesi, *Phys. Lett. B* **406**, 237 (1997).
- [20] W. Buchmüller and D. Wyler, *Phys. Lett. B* **407**, 147 (1997).